


RESEARCH ARTICLE

Open Access



# Molecular characterization of carbendazim resistance of *Fusarium* species complex that causes sugarcane pokkah boeng disease

Shiqiang Xu<sup>1†</sup>, Jihua Wang<sup>1,2†</sup>, Haixuan Wang<sup>1†</sup>, Yixue Bao<sup>1†</sup>, Yisha Li<sup>1</sup>, Muralidharan Govindaraju<sup>1</sup>, Wei Yao<sup>1</sup>, Baoshan Chen<sup>1</sup> and Muqing Zhang<sup>1\*</sup> 

## Abstract

**Background:** Pokkah boeng is one of the most serious and devastating diseases of sugarcane and causes significant loss in cane yield and sugar content. Although carbendazim is widely used to prevent fungal diseases, the molecular basis of *Fusarium* species complex (FSC) resistance to carbendazim remains unknown.

**Results:** The EC<sub>50</sub> (fungicide concentration that inhibits 50% of mycelial growth) values of carbendazim for 35 FSC isolates collected in cane growing regions of China were ranged from 0.5097 to 0.6941 μg mL<sup>-1</sup> of active ingredient (a.i.), in an average of 0.5957 μg a.i. mL<sup>-1</sup>. Among carbendazim-induced mutant strains, SJ51M (*F. verticillioides*) had a CTG rather than CAG codon (Q134L) at position 134 of the FVER\_09254 gene, whereas in the mutant strain HC30M (*F. proliferatum*) codon ACA at position 351 of the FPRO\_07779 gene was replaced by ATA (T351I). Gene expression profiling analysis was performed for SJ51M and its corresponding wild type strain SJ51, with and without carbendazim treatment. The gene expression patterns in SJ51 and SJ51M changed greatly as evidenced by the detection of 850 differentially expressed genes (DEGs). Functional categorization indicated that genes associated with oxidation-reduction process, ATP binding, integral component of membrane, transmembrane transport and response to stress showed the largest expression changes between SJ51M and SJ51. The expression levels of many genes involved in fungicide resistance, such as detoxification enzymes, drug efflux transporters and response to stress, were up-regulated in SJ51M compared to SJ51 with and without carbendazim treatment.

**Conclusion:** FSC was sensitive to carbendazim and had the potential for rapid development of carbendazim resistance. The transcriptome data provided insight into the molecular pathways involved in FSC carbendazim resistance.

**Keywords:** Pokkah boeng, *Fusarium verticillioides*, *Fusarium proliferatum*, Carbendazim-induced mutant, Gene expression profile

## Background

Pokkah boeng disease caused by FSC was firstly recognized more than 100 years ago and is a devastating disease that affects sugarcane production worldwide [1–3]. In recent years, pokkah boeng disease has become increasingly severe in China. Pokkah boeng causes serious yield losses (about 10–40%) in commercial sugarcane production. Disease outbreaks in susceptible cultivars

have been reported in Yunnan, China and Shahjahanpur, India [2, 4]. The characteristic symptoms manifest as chlorosis, twisting and shortening of young leaves as well as stalk rot. Many *Fusarium* species, such as *F. moniliformae*, *F. sacchari*, *F. verticillioides* and *F. moniliforme* var. *subglutinans*, have been reported as causal organisms of pokkah boeng disease [2, 5–7]. *F. verticillioides* and *F. proliferatum* are two major *Fusarium* species that cause sugarcane pokkah boeng disease in China, with *F. verticillioides* accounting for over 90% of the recorded disease [8].

Methyl benzimidazole carbamate (MBC) fungicides, particularly carbendazim, a broad spectrum fungicide, provide effective control of fungal diseases in a variety of

\* Correspondence: [mqzhang@ufl.edu](mailto:mqzhang@ufl.edu)

<sup>†</sup>Shiqiang Xu, Jihua Wang, Haixuan Wang and Yixue Bao contributed equally to this work.

<sup>1</sup>State Key Lab for Conservation and Utilization of Subtropical Agric-Biological Resources, Guangxi University, Nanning 530005, China

Full list of author information is available at the end of the article



crops. Carbendazim can prevent pokkah boeng disease, especially in the top rot phase infection [9]. In China, carbendazim has been widely used to control pokkah boeng disease since 1980s, especially in chewing cane. However, carbendazim cannot be continuously applied to prevent pokkah boeng disease in chewing cane fields due to the development of resistant FSC. In our field survey, about 15% of carbendazim-resistant FSC was seen with carbendazim  $EC_{50}$  of  $1.86 \mu\text{g a.i. mL}^{-1}$  in a chewing cane field in Guangzhou, China, indicating that repeated and intensive applications of carbendazim could have promoted emergence of resistant FSC strains in this region. Thus, investigation of carbendazim sensitivity in FSC isolates from sugarcane planting areas in China is essential to assess the risk of carbendazim resistance.

MBC fungicides inhibit mitosis by binding to  $\beta$ -tubulin and inhibiting tubulin biosynthesis [10, 11]. MBC-resistant strains have been reported in many phytopathogenic fungi [12–15]. Point mutations in  $\beta$ -tubulin 2 (*Tub2*) can confer MBC resistance by altering amino acids in the MBC binding site [16]. Substitutions at codons 6, 50, 134, 165, 167, 198, 200, 235, 240, 241 and 257 in the *Tub2* gene have been shown to cause MBC resistance in field or laboratory isolates of several pathogenic fungi [16–19]. However, several exceptions have been reported wherein mutations that cause changes in *Tub2* amino acid sequences are not detected in several resistant strains, suggesting that there may be other pathways involved in the molecular mechanism of MBC resistance [20, 21].

Indeed, fungicide resistance can also be induced through various mechanisms, mainly structural alterations in target sites that reduce fungicide affinity, overexpression of fungicide target genes and metabolic decomposition and active efflux to reduce intracellular fungicide concentration [16, 22]. The development of genomic, proteomic, transcriptomic and bioinformatics provides a new strategy for exploring fungicide resistance mechanisms. RNA sequencing (RNA-seq) is an effective method to identify responses at the gene expression level and has been widely used in the research of resistance mechanisms. Indeed, transcriptome data reveal that *Trichophyton rubrum* response to acriflavine-involved genes categorize as oxidation-reduction reaction, transmembrane transport, and metal ion binding [23]. Genes encoding proteins involved in drug efflux confer *Penicillium digitatum* prochloraz resistance. These genes include transporters of the major facilitator superfamily (MFS), ATP-binding cassette transporters and the multidrug and toxic compound extrusion family [24].

The molecular basis of FSC resistance to carbendazim in different sugarcane planting areas around China is unclear, and carbendazim-resistant mutants have not been characterized. Therefore, the objectives of this study were to: (i) determine the carbendazim sensitivity of FSC isolates from different sugarcane planting areas around

China, (ii) carry out a preliminary assessment of the risk of FSC resistance to carbendazim and characterize the carbendazim-induced mutants and (iii) understand the molecular mechanisms that could promote the development of carbendazim resistance in FSC.

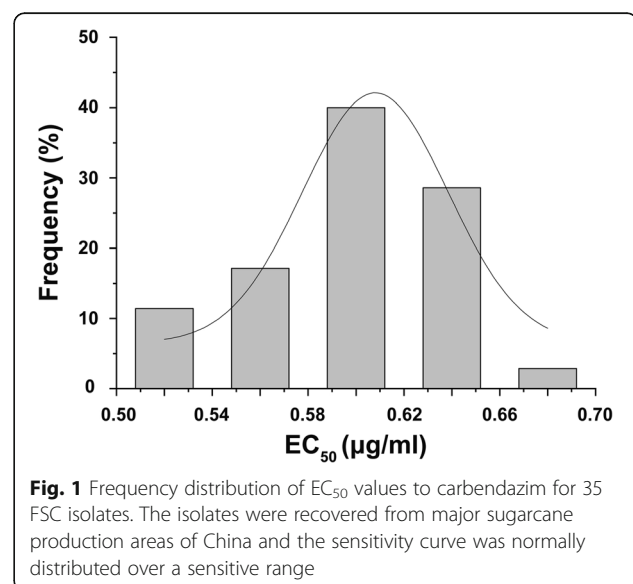
## Results

### Sensitivity of FSC to Carbendazim

None of the 35 FSC isolates grew on potato dextrose agar (PDA) amended with  $1.2 \mu\text{g a.i. mL}^{-1}$  carbendazim, but at  $1.1 \mu\text{g a.i. mL}^{-1}$  carbendazim, three isolates grew slowly (1 to 3 mm colony diameter). The carbendazim  $EC_{50}$  values for the 35 isolates ranged from  $0.5097$  to  $0.6941 \mu\text{g a.i. mL}^{-1}$  with an average  $EC_{50}$  of  $0.5957 \mu\text{g a.i. mL}^{-1}$  (Additional file 1: Table S1), indicating that these FSC isolates were susceptible to carbendazim. The normal distributions of  $EC_{50}$  of these isolates indicated that the  $0.5957 \mu\text{g a.i. mL}^{-1}$  was a suitable threshold concentration to assess carbendazim resistance in the subsequent experiments (Fig. 1).

### Carbendazim-induced mutants in vitro

Isolates exposed to different carbendazim concentrations were continuously cultured at  $28^\circ\text{C}$  in the dark to induce the rapid growth of mutants, which grew in a fan shape at the edge of some colonies. The earliest appearance of a mutant area occurred at the edge of a SJ51 colony on day 5 of culture (Fig. 2a). After 14 days of culture, 18 fan-shaped mutant areas were obtained from 14 strains at carbendazim concentrations ranging from  $0.6$  to  $0.9 \mu\text{g a.i. mL}^{-1}$ . Three mutants were obtained from strain DH19, two from HC35 and LW54, and only one from the other 11 tested isolates. Carbendazim sensitivity of these mutants was measured after sub-culturing for 10 continuous generations on



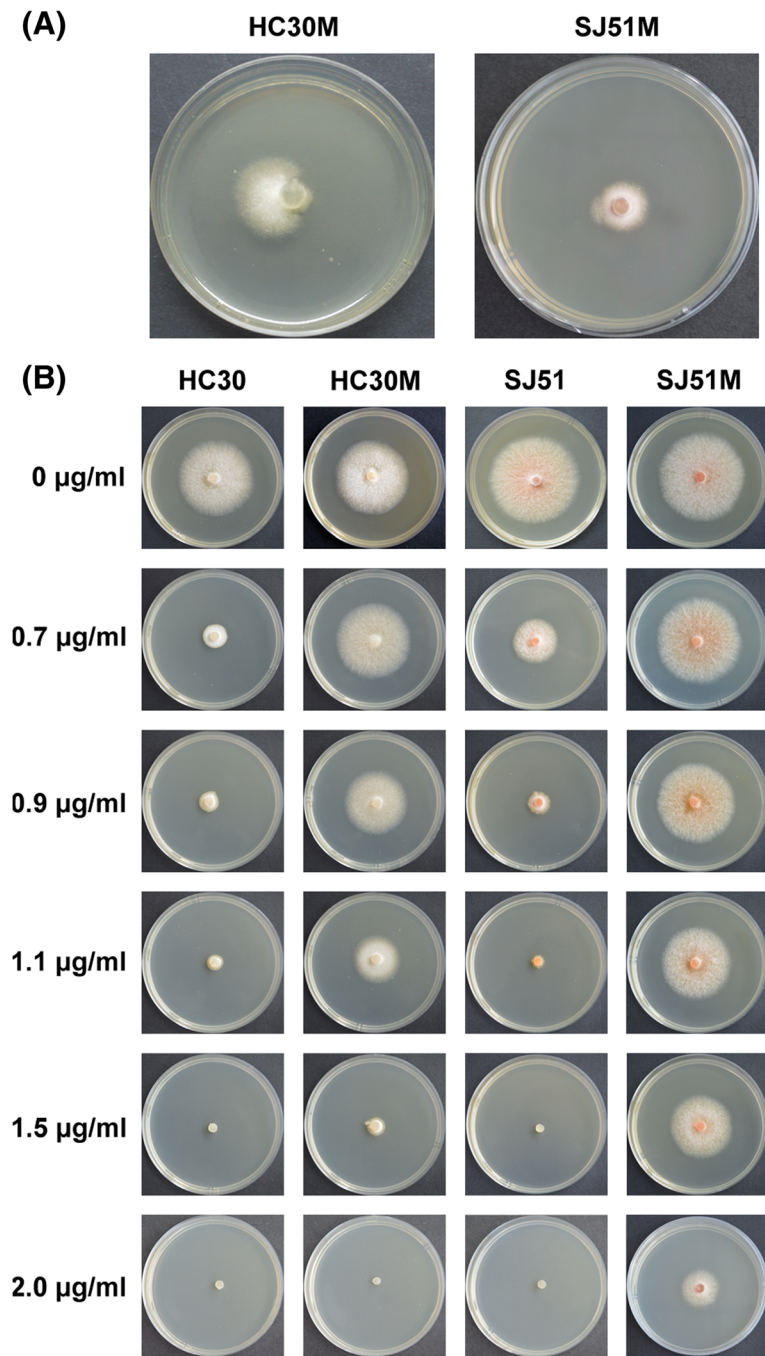


**Fig. 2** Colony morphology of FSC wild types and their mutants. **(a)** The fan-shaped region on the edge of the colony induced by carbendazim of SJ51 (on day 5) and HC30 (on day 8); **(b)** Mycelial growth of two FSC strains and their resistant mutants exposed to carbendazim. All strains were grown at 28 °C for 3 days on PDA media amended with carbendazim at 0, 0.7, 0.9, 1.1, 1.5 or 2.0 µg a.i.mL<sup>-1</sup>

carbendazim-free PDA medium. Five mutants had higher and more stable resistance to carbendazim with EC<sub>50</sub> > 1.0 µg a.i. mL<sup>-1</sup>, whereas another 13 mutants had EC<sub>50</sub> values that were similar to those for the wild type (Additional file 2: Table S2). The fan-shaped region and colony morphology exposed to different concentration of carbendazim of SJ51M and HC30M were presented in Fig. 2.

**Detection of mutations in *Tub2* genes in carbendazim mutants**

Genome sequencing of *F. verticillioides* CNO-1 showed two genes encoding *Tub2* (FVER\_05465 and FVER\_09254). The coding regions of FVER\_05465 had 1341 nucleotides encoding 446 amino acids, which had 100% homology to *F. sacchari* FRC R-6865 *Tub2*

(GenBank accession number KU171789.1). Meanwhile, the coding regions of FVER\_09254 included 1347 nucleotides that encode 448 amino acids, which were 99% homologous to that of *F. fujikuroi* (GenBank accession number AHG97571.1). *Tub2* DNA sequences were amplified and sequenced from five carbendazim-resistant mutants (SJ51M, HC30M, FZ15M, YN54M and FN22M) and the corresponding wild type strains. In the FVER\_09254 gene from SJ51M, the CAG codon at position 134 was replaced by CTG (Q134L; A/T transition), whereas in mutant HC30M the codon ACA at position 351 of FPRO\_07779 was replaced by ATA (T351I; C/T transversion) (Additional file 3: Figure S1). No point mutations in FVER\_09254 and FVER\_05465 were detected in the FZ15M, YN54M and FZ22M mutants.

**Temperature response and pathogenicity of carbendazim resistant mutants**

The *Tub2* mutants were tested for their ability to grow at various temperatures with and without carbendazim. After culturing for 5 days, SJ51M grew at all tested temperatures (15 °C, 28 °C, 34 °C and 37 °C) on PDA with 1.9 µg a.i. mL<sup>-1</sup> carbendazim (nearly equal to EC<sub>50</sub> of SJ51M), but wild type SJ51 failed to grow. The mutant HC30M grew at 28 °C and 34 °C on PDA amended with 1.2 µg a.i. mL<sup>-1</sup> carbendazim (nearly equal to EC<sub>50</sub> of HC30M), whereas wild type HC30 failed to grow. Neither the mutant HC30M nor its wild type counterpart HC30 grew at 15 °C on PDA medium with carbendazim but did grow on PDA without carbendazim, whereas HC30M showed little growth at 37 °C in the presence or absence of carbendazim, similar to the growth of HC30 in absence of carbendazim (Additional file 4: Table S3). After culturing for 5 days at 28 °C on PDA medium, the radial growth (colony diameter) and colony morphology of SJ51M and HC30M were similar to wild type SJ51 and HC30 (Additional file 5: Figure S2). In pathogenicity assays, sugarcane plants inoculated with mutant (SJ51M and HC30M) or corresponding wild type strains (SJ51 and HC30) showed typical symptoms (e.g., growth point rot) 10 days after inoculation, while the control plants remained asymptomatic (Additional file 5: Figure S2). These results indicated that *Tub2* point mutations did not affect the growth and pathogenicity of the SJ51M and HC30M mutants.

**Gene expression profiles of carbendazim-resistant mutants exposed to carbendazim in vitro**

Gene expression changes in the carbendazim-resistant mutant SJ51M and wild-type SJ51 exposed to carbendazim were explored by Illumina sequencing. More than 229 million high-quality reads were generated from the samples and over 75% of the total reads mapped to the *F. verticillioides* CNO-1 genome (Additional file 6: Table S4).

These data were deposited in the Sequence Read Archive (SRA) in the GenBank database under accession number SRP127969. Both SJ51 and the carbendazim-resistant mutant SJ51M grew on potato dextrose broth (PDB) medium amended with the corresponding carbendazim EC<sub>50</sub> (1.87 a.i. mL<sup>-1</sup> and 0.61 a.i. mL<sup>-1</sup> for SJ51M and SJ51, respectively). A total of 290 DEGs were detected in SJ51M, including 225 and 65 that were up- and down-regulated, respectively. Wild type SJ51 showed 183 DEGs, including 135 up-regulated and 48 down-regulated genes (Table 1). SJ51 and SJ51M shared 75 DEGs after carbendazim exposure, whereas 215 unique DEGs were detected in mutant SJ51M and wild type SJ51 had 108 unique DEGs (Fig. 3a and b). Overall, 456 and 350 DEGs were detected between SJ51 and SJ51M with and without carbendazim treatment, respectively (Table 1 and Fig. 3). These results demonstrated that the gene expression patterns for SJ51 and SJ51M changed significantly under both normal conditions and carbendazim treatment, suggesting that some mechanisms may be specific to the development of carbendazim resistance.

To characterize how mutations in SJ51M affect carbendazim resistance, gene ontology (GO) enrichment analysis of the DEGs was performed using Goseq R packages (Additional file 7: Table S5). The function categories of oxidation-reduction process, ATP binding, integral component of membrane, transmembrane transport and response to stress were the most abundant in SJ51M relative to wild type SJ51. These results indicated that both energy metabolism and membrane stability/permeability were significantly affected by carbendazim. Most DEGs related to transmembrane transport (Fig. 4a) and response to stress (Fig. 4b) showed higher transcript levels in SJ51M compared to SJ51 under both normal conditions and in the presence of carbendazim treatment. To elucidate the similarities and differences in the expression pattern of the DEGs in the four treatments, a hierarchical clustering analysis was performed (Fig. 5a). The expression patterns of 850 DEGs could be divided into 12 clusters, suggestive of differences between SJ51M and SJ51 in response to

**Table 1** Number of DEGs in SJ51M and its corresponding wild type strain SJ51

| DEG Set            | All DEGs | Up-regulated DEGs | Down-regulated DEGs |
|--------------------|----------|-------------------|---------------------|
| SJ51_E vs SJ51_C   | 183      | 135               | 48                  |
| SJ51M_E vs SJ51M_C | 290      | 225               | 65                  |
| SJ51M_C vs SJ51_C  | 350      | 183               | 167                 |
| SJ51M_E vs SJ51_E  | 456      | 278               | 178                 |

SJ51\_C and SJ51M\_C represented without carbendazim treatment, while SJ51\_E and SJ51M\_E represented exposed to carbendazim treatment. The cut-off limit of DEGs was less than 0.05 FDR and greater than 2-fold change

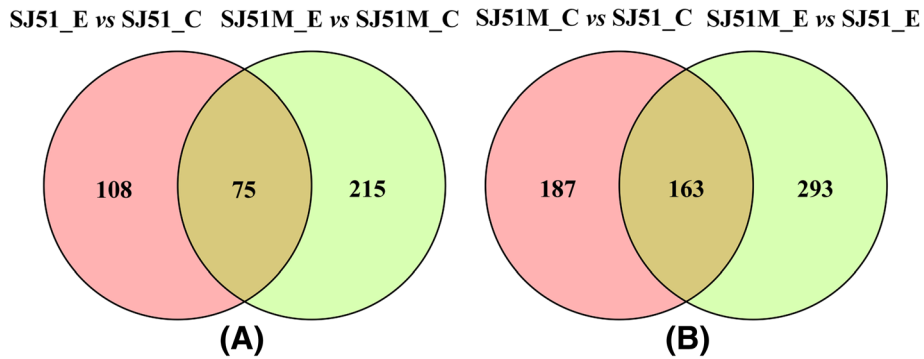


**Fig. 3** Venn diagrams showing the number of DEGs in SJ51M and its corresponding wild type strain SJ51. (a) The number of unique and shared DEGs of SJ51M and SJ51 responding to carbendazim treatment; (b) The number of unique and shared DEGs between SJ51M and SJ51 with and without carbendazim treatment. SJ51\_C and SJ51M\_C represented without carbendazim treatment, while SJ51\_E and SJ51M\_E represented exposed to carbendazim treatment. The cut-off limit of DEGs was less than 0.05 FDR and greater than 2-fold change

carbendazim pressure. We focused our attention on the five clusters that contained genes with increased expression in SJ51M\_E that were likely related to carbendazim resistance (cluster numbers I, II, III, IX and X, respectively). In cluster I (Fig. 5b), 143 genes had increased expression in SJ51M relative to SJ51 after exposure to carbendazim, including three genes (FVER\_03030, FVER\_09237 and FVER\_11289) encoding the ABC multidrug transporter, which is critical for transmembrane transport during drug efflux. Nine genes belong to MFS, one of which encodes caffeine resistance protein 5 and

two encode the HC-toxin efflux carrier TOXA. Increased expression was seen for FVER\_09899, encoding a glutathione S-transferase that is important for fungicide detoxification. In addition, a group of genes related to response to stress and oxidative stress were identified in this cluster, and included heat shock protein, catalase and thioredoxin. In cluster II, IX and X (Fig. 5c, e and f), several genes were highly expressed during exposure of SJ51M to carbendazim, notably genes related to transmembrane transport, including four genes encoding the MFS transporter and one encoding the ABC transporter

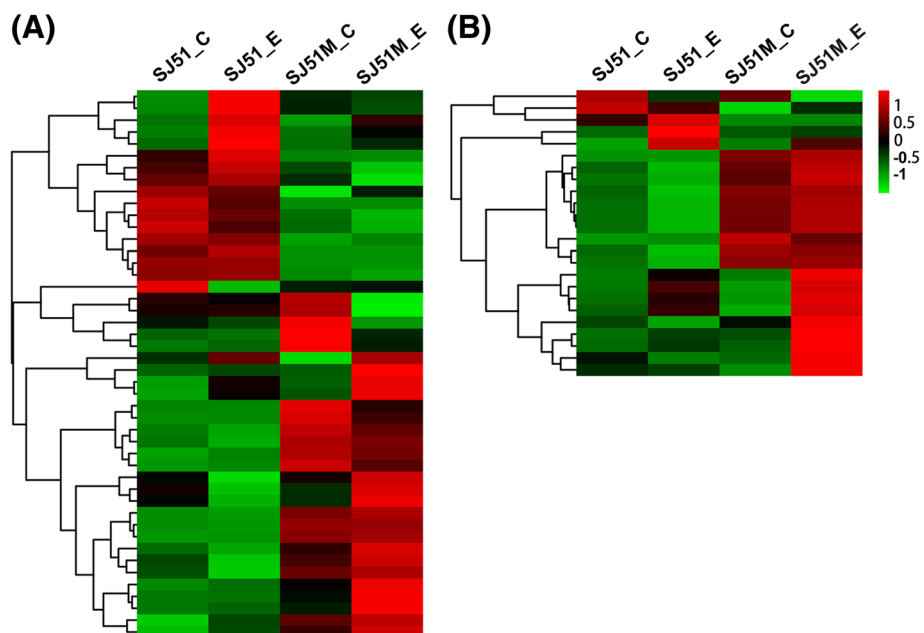
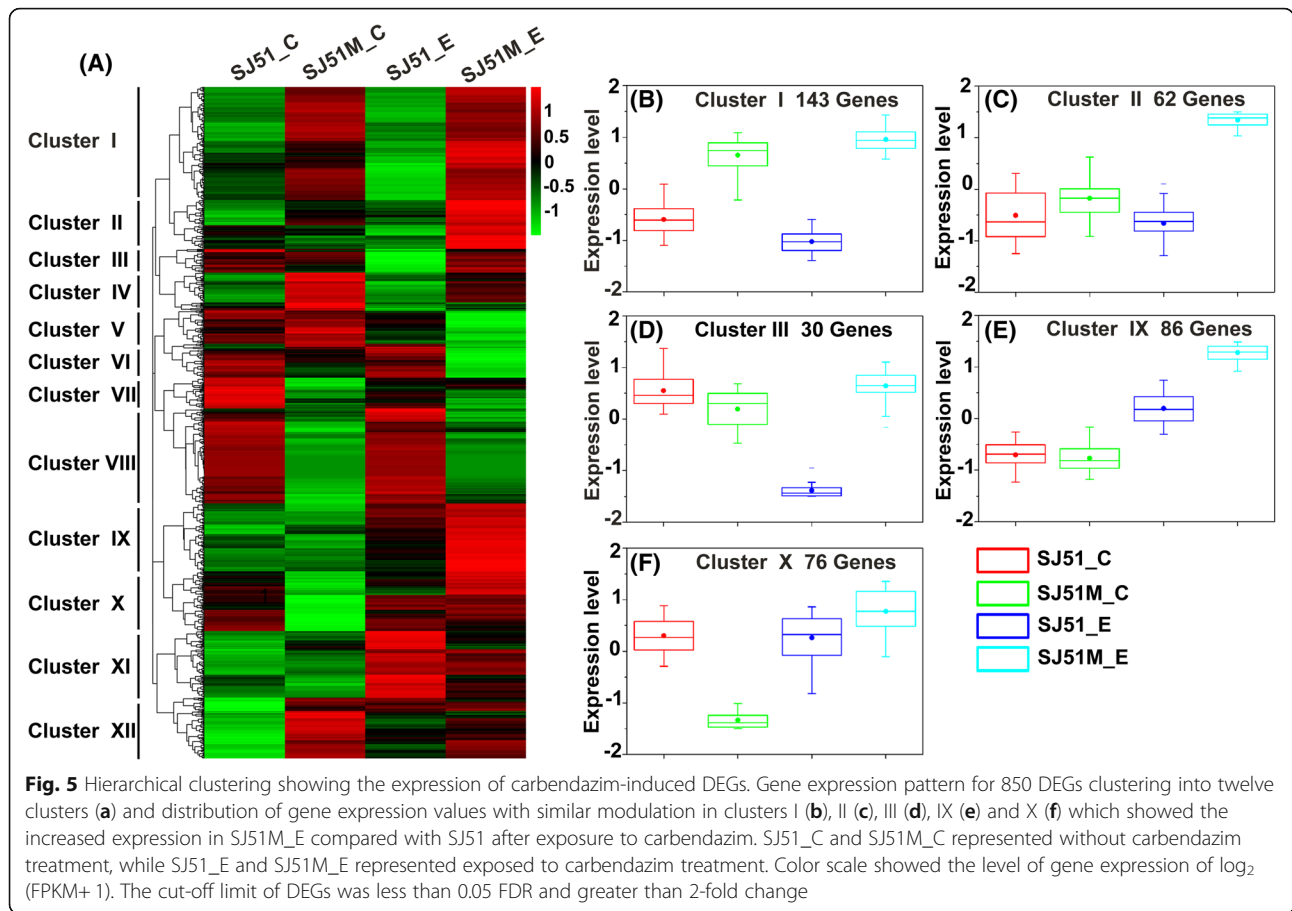


**Fig. 4** Heatmaps showing the expression pattern of DEGs. The expression pattern of DEGs related to transmembrane transport (GO:0055085) (a) and response to stress (GO:0006950) (b). SJ51\_C and SJ51M\_C represented without carbendazim treatment, while SJ51\_E and SJ51M\_E represented exposed to carbendazim treatment. Color scale showing the level of gene expression of  $\log_2$  (FPKM+ 1). The cut-off limit of DEGs was less than 0.05 FDR and greater than 2-fold change



in cluster II. Two genes (FVER\_05972 and FVER\_12450) were related to glyoxalase/bleomycin resistance protein/dioxygenase superfamily in cluster IX. After exposure to carbendazim, FVER\_12450 expression increased 3.19-fold in SJ51, whereas expressions of FVER\_12450 and FVER\_05972 showed increases of 10.77- and 16.11-fold in SJ51M, respectively. Intriguingly, two genes (FVER\_08360 and FVER\_05071) in cluster X that were related to the kinesin family play a critical role in mitosis by mediating microtubule assembly. Thirty genes in cluster III (Fig. 5d) had strongly decreased expression in wild type SJ51 upon exposure to carbendazim, but showed slightly up-regulated expression in the resistant mutant SJ51M, indicating that several cellular processes kept normal at the mutants of SJ51M exposed to carbendazim. In this cluster, FVER\_09965 encoding kinesin-related protein KIP3, and FVER\_14552 encoding GTPase-binding protein rid1, were observed.

**Quantitative real-time PCR (qRT-PCR) validation of target genes**

The RNA-seq results were validated using qRT-PCR for ten genes selected for their involvement in transmembrane transport, oxidoreductase activity, response to stress

and the target gene of carbendazim, including three ABC multidrug transporters (FVER\_03030, FVER\_09560 and FVER\_11289), a MFS-type transporter (FVER\_11009), four heat shock proteins (FVER\_02883, FVER\_03117, FVER\_09151 and FVER\_10345), a thioredoxin protein (FVER\_11010) and the target gene *Tub2* (FVER\_09254). Among these genes, expression of FVER\_11009 (Fig. 6a) was up-regulated in SJ51M after carbendazim treatment, while expression of FVER\_09151 (Fig. 6b) was down-regulated and FVER\_09254 (Fig. 6c) was up-regulated in SJ51. FVER\_11010 expression was up-regulated in SJ51M relative to SJ51 exposed to carbendazim (Fig. 6d). Three ABC multidrug transporters, the MFS-type transporter and four heat shock proteins were all up-regulated in SJ51M compared to SJ51 (Fig. 6a and b). The correlation between RNA-Seq and qRT-PCR was statistically significant ( $r = 0.88, p < 0.001$ ) (Fig. 6e), suggesting that the transcriptome data were reliable and could provide a basis to explore the mechanism of FSC carbendazim resistance.

**Discussion**

Carbendazim-resistant strains have been identified in chewing cane, which is widely used to prevent pokkah

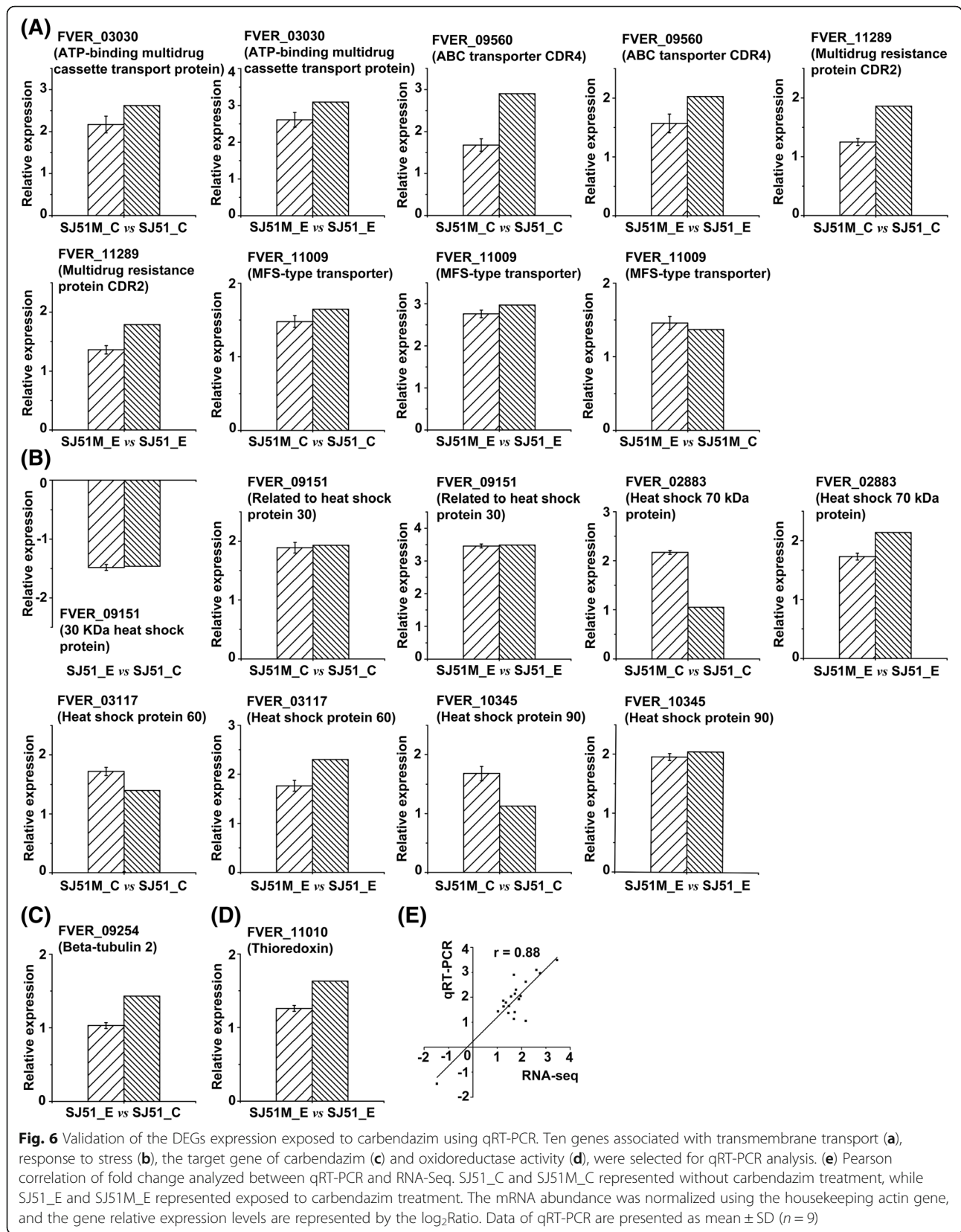


**Fig. 6** Validation of the DEGs expression exposed to carbendazim using qRT-PCR. Ten genes associated with transmembrane transport (a), response to stress (b), the target gene of carbendazim (c) and oxidoreductase activity (d), were selected for qRT-PCR analysis. (e) Pearson correlation of fold change analyzed between qRT-PCR and RNA-Seq. SJ51\_C and SJ51M\_C represented without carbendazim treatment, while SJ51\_E and SJ51M\_E represented exposed to carbendazim treatment. The mRNA abundance was normalized using the housekeeping actin gene, and the gene relative expression levels are represented by the log<sub>2</sub>Ratio. Data of qRT-PCR are presented as mean ± SD (n = 9)

boeng disease [25]. Here we tested 35 FSC isolates recovered from major sugarcane production areas of China. To our knowledge, this is the first report to assess carbendazim sensitivity of FSC collected from different locations in China. All strains in this study were sensitive to carbendazim, with  $EC_{50}$  values ranging from 0.5097 to 0.6941  $\mu\text{g a.i. mL}^{-1}$  and a mean of 0.5957  $\mu\text{g a.i. mL}^{-1}$  (Additional file 1: Table S1). These results were similar to those for *Gibberella zeae* (a *F. graminearum* teleomorph), a carbendazim-sensitive strain having a mean  $EC_{50}$  value of 0.59  $\mu\text{g a.i. mL}^{-1}$  [26]. No resistant strains were detected in our collected isolates because carbendazim was more commonly used to treat seed cane prior to planting rather than for manual foliar application during the early stage of field production, such that mostly 3–7 month old sugarcane is infected in China. More strains will be collected and recovered from the field samples to test their sensitivity to carbendazim. With the higher incidence, few resistant cultivars were available, thus fungicides are needed to prevent pokkah boeng disease. Carbendazim was effective against pokkah boeng disease and had the lowest  $EC_{50}$  value relative to other fungicides (e.g., dimethachlon, chlorothalonil, mancozeb and Meroif<sup>™</sup>) [27]. Based on this analysis, it was presumed that carbendazim could be widely used to prevent pokkah boeng disease in China.

Carbendazim resistance develops rapidly in many pathogenic fungi [12–15]. Under selection pressure of fungicides, resistant strains can adapt to environmental conditions to become the major strain in pathogen populations, and in turn decrease fungicide effectiveness [16]. Although UV irradiation was widely used to select for fungicide resistance, in this study we instead used fungicide-induced mutations to assess the risk from emergence of resistant strains because mutants might better represent those that arise following fungicide application in the field. Here, fan-shaped growth of 18 mutants was induced at the edge of 14 isolates. After stability and sensitivity testing, the  $EC_{50}$  of the five mutant strains (SJ51M, HC30M, FN22M, YN54M and FZ15M) exceeded 1.0  $\mu\text{g a.i. mL}^{-1}$ , which was higher than that of the corresponding wild type strain, and in the case of SJ51M, the difference in  $EC_{50}$  was 3-fold (Additional file 2: Table S2 and Fig. 2). A single application of carbendazim could quickly induce resistant strains in vitro, indicating that FSC can easily develop carbendazim resistance, even if the resistance level of the resistant isolates was not high. Compared to the other pathogenic fungi, strains of *F. graminearum* with a minimum inhibitory concentration of over 1.4  $\mu\text{g mL}^{-1}$  carbendazim were regarded as resistant isolates [14]. We observed similar trends in resistance level in mutant strains of FSC, which may be related to the characteristics of FSC.

The mechanism of resistance to carbendazim was associated with point mutations in the *Tub2* gene that change the structure of the fungicide binding site to decrease sensitivity in turn [16, 28]. According to the genome sequencing information, *F. verticillioides* CNO-1 has two homologous *Tub2* genes. A point mutation at codon 134 (Q134L) was detected in FVER\_09254 from the resistant strain SJ51M; a similar mutation was reported in a laboratory-induced mutant of *Aspergillus nidulans* that had a mutation at codon 134 (Q134K) and was sensitive to heat, which could interfere with fitness under field conditions [17]. SJ51M with a mutation site at codon 134 was not heat sensitive and grew at 34 and 37 °C on PDA amended with carbendazim (Additional file 3: Figure S1 and Additional file 4: Table S3). A novel point mutation at codon 351 (T351I) was detected in FPRO\_07779 in mutant HC30M (Additional file 3: Figure S1). A point mutation at codon 351 in the *Tub2* gene that confers carbendazim resistance has not been reported in other phytopathogenic fungi, either in field or laboratory isolates. The mutant HC30M carrying a mutation at codon 351 was cold sensitive and showed no resistance to carbendazim at 15 °C (Additional file 4: Table S3). We also confirmed the absence of mutations in the *Tub2* sequence in the resistant strains FN22M, YN54M and FZ15M. These results indicated that other mechanisms must be involved in FSC carbendazim resistance. The virulence of resistant isolates SJ51M and HC30M both induced disease to similar levels relative to the corresponding wild type strains SJ51 and HC30, respectively. Similar studies describing isolates of carboxin-resistant *Ustilago nuda* and boscalid-resistant *Alternaria alternata* also showed that the pathogenicity of these mutants was not significantly altered on *Hordeum vulgare* and *Pistachio*, respectively [29, 30].

Kinesins play important roles in transporting organelles and vesicles along microtubules and participate in cell mitosis [31]. The disorder of microtubule cytoskeleton and actin cytoskeleton affected mycelial growth and led to cell death in *F. graminearum* [32]. Interestingly, several genes involved in the kinesin family have been implicated in fungicide resistance. Here, expression of FVER\_09965 (in cluster III) was sharply down-regulated in SJ51 but was slightly up-regulated in SJ51M after exposure to carbendazim. Expressions of FVER\_05071, FVER\_08360 and FVER\_10733 were up-regulated in SJ51 and SJ51M after exposure to carbendazim, but the up-regulation was more pronounced in SJ51M (Table 2). These data indicated that *Tub2* mutations might affect microtubule structure that in turn affected kinesin function, especially after carbendazim treatment. Small GTPase family regulate a variety of signal transduction pathways, such as cytoskeletal formation and protein trafficking and endocytosis, which may play important



**Table 2** The major genes modulated in SJ51M and its corresponding wild type strain SJ51 after carbendazim exposure

| Gene ID    | Log <sub>2</sub> (Fold change) |                      |                      |                      | Gene annotation   |
|------------|--------------------------------|----------------------|----------------------|----------------------|---|
|            | SJ51_E vs SJ51_C               | SJ51M_E vs SJ51M_C   | SJ51M_C vs SJ51_C    | SJ51M_E vs SJ51_E    |   |
| FVER_05972 | -                              | 4.0095 <sup>a</sup>  | -                    | 2.2519 <sup>a</sup>  | Glyoxalase/Bleomycin resistance protein/Dioxygenase superfamily |
| FVER_12450 | 1.6720 <sup>a</sup>            | 3.4288 <sup>a</sup>  | 0.1681               | 1.9312 <sup>a</sup>  | Glyoxalase/Bleomycin resistance protein/Dioxygenase superfamily |
| FVER_11289 | -0.1793                        | -0.2528              | 1.8589 <sup>a</sup>  | 1.7887 <sup>a</sup>  | Multidrug resistance protein CDR2                               |
| FVER_09237 | -0.6985                        | 0.6653               | 1.0074               | 2.2519 <sup>a</sup>  | Multidrug resistance protein fnx1                               |
| FVER_12798 | -0.3570                        | -1.5140 <sup>a</sup> | 0.7393               | -0.4143              | Multidrug resistance protein CDR1                               |
| FVER_09560 | 0.0170                         | -0.8521              | 2.8984 <sup>a</sup>  | 2.0326 <sup>a</sup>  | ABC transporter CDR4  |
| FVER_04236 | -0.0264                        | -0.4497              | 1.0549 <sup>a</sup>  | 0.6350               | Probable MFS multidrug resistance transporter                   |
| FVER_10334 | 2.5884 <sup>a</sup>            | 1.2424               | 1.3038               | -0.0260              | Pleiotropic ABC efflux transporter of multiple drugs            |
| FVER_03030 | -0.3064                        | 0.1645               | 2.6240 <sup>a</sup>  | 3.0980 <sup>a</sup>  | Related to ATP-binding multidrug cassette transport protein     |
| FVER_05891 | 0.0651                         | -0.3041              | 1.2302 <sup>a</sup>  | 0.8643               | Probable ATP-binding multidrug cassette transport protein       |
| FVER_03551 | 0.1228                         | 1.1575 <sup>a</sup>  | 0.2902               | 1.3278 <sup>a</sup>  | ABC transporter ATP-binding protein                             |
| FVER_11889 | -0.3146                        | 0.0465               | 2.5807 <sup>a</sup>  | 2.8235 <sup>a</sup>  | Caffeine resistance protein 5                                   |
| FVER_01165 | 2.6628 <sup>a</sup>            | 2.3188 <sup>a</sup>  | 1.3811               | 1.0704 <sup>a</sup>  | Metal resistance protein YCF1                                   |
| FVER_03117 | -0.9540                        | -0.0568              | 1.4012 <sup>a</sup>  | 2.3016 <sup>a</sup>  | Heat shock protein 60, mitochondrial                            |
| FVER_04661 | -0.7160                        | 0.4776               | 1.2237 <sup>a</sup>  | 2.4205 <sup>a</sup>  | Heat shock protein 78, mitochondrial                            |
| FVER_04571 | -0.6983                        | 0.2399               | 1.1257 <sup>a</sup>  | 2.0672 <sup>a</sup>  | Probable heat shock protein HSP104                              |
| FVER_12593 | -0.3875                        | 0.1239               | 0.9569               | 1.4716 <sup>a</sup>  | Heat shock protein sti1 homolog                                 |
| FVER_02883 | -0.7821                        | 0.3016               | 1.0488 <sup>a</sup>  | 2.1358 <sup>a</sup>  | Heat shock 70 kDa protein                                       |
| FVER_09674 | 0.0077                         | 0.1043               | 0.9416               | 1.0415 <sup>a</sup>  | Heat shock 70 kDa protein                                       |
| FVER_01860 | -1.1244 <sup>a</sup>           | 0.5785               | 0.9860               | 2.6906 <sup>a</sup>  | Probable FES1-Hsp70 nucleotide exchange factor                  |
| FVER_11673 | -0.9108                        | 0.6567               | 0.7528               | 2.3235 <sup>a</sup>  | Heat shock 70 kDa protein                                       |
| FVER_10345 | -0.6977                        | 0.2154               | 1.1314 <sup>a</sup>  | 2.0537 <sup>a</sup>  | Heat shock protein 90   |
| FVER_09151 | -1.4554 <sup>a</sup>           | 0.1075               | 1.9281 <sup>a</sup>  | 3.4943 <sup>a</sup>  | Related to heat shock protein 30                                |
| FVER_04255 | 0.1770                         | -0.5574              | 1.1400 <sup>a</sup>  | 0.4186               | Probable chaperone protein HSP31                                |
| FVER_08232 | -0.2435                        | 0.5509               | -1.0321 <sup>a</sup> | -0.2344              | Catalase  |
| FVER_08876 | -0.1428                        | 0.4837               | 1.5837 <sup>a</sup>  | 2.2136 <sup>a</sup>  | Catalase  |
| FVER_11010 | -0.6185                        | 0.1034               | 0.9058               | 1.6309 <sup>a</sup>  | Thioredoxin   |
| FVER_02416 | -0.1779                        | 2.1616 <sup>a</sup>  | -0.1494              | 2.1632 <sup>a</sup>  | Related to thioredoxin reductase                                |
| FVER_07248 | -0.6687                        | -0.7614              | 1.1560 <sup>a</sup>  | 1.0657 <sup>a</sup>  | Related to DSBA-like thioredoxin domain protein                 |
| FVER_13986 | 0.4550                         | 1.4076 <sup>a</sup>  | 0.3056               | 1.2617 <sup>a</sup>  | Related to cytosolic Cu/Zn superoxide dismutase                 |
| FVER_05859 | 1.2131 <sup>a</sup>            | 0.5427               | 1.2630 <sup>a</sup>  | 0.5976               | Cytochrome P450 52A3-A  |
| FVER_11192 | -0.0087                        | 0.0414               | 1.6595 <sup>a</sup>  | 1.7130 <sup>a</sup>  | Cytochrome P450 52A6  |
| FVER_08550 | 1.0365                         | -1.0307              | 2.2312 <sup>a</sup>  | 0.1358               | Related to Glutathione S-transferase II                         |
| FVER_09899 | 0.0960                         | -0.2003              | 1.5924 <sup>a</sup>  | 1.2997 <sup>a</sup>  | Related to microsomal glutathione S-transferase 3               |
| FVER_00097 | -0.4491                        | -0.5106              | 1.4609 <sup>a</sup>  | 1.4023 <sup>a</sup>  | Glutathione S-transferase                                       |
| FVER_09254 | 1.4333 <sup>a</sup>            | 0.3586               | 0.2223               | -0.8490              | Beta-tubulin 2  |
| FVER_09965 | -1.6756 <sup>a</sup>           | 0.3958               | -1.3325              | 0.7231               | Probable kinesin-related protein KIP3                           |
| FVER_10733 | 3.9528 <sup>a</sup>            | 2.0084 <sup>a</sup>  | 0.1825               | -1.7512 <sup>a</sup> | Kinesin-like protein KIP3                                       |
| FVER_05071 | 0.2857                         | 1.1278 <sup>a</sup>  | -0.7088              | 0.1354               | Kinesin-like protein klpA                                       |
| FVER_08360 | 0.6639                         | 3.7064 <sup>a</sup>  | -1.4850 <sup>a</sup> | 1.5549 <sup>a</sup>  | Kinesin family member 1/13/14                                   |
| FVER_00402 | -0.3106                        | 1.6102 <sup>a</sup>  | -0.6439              | 1.2774 <sup>a</sup>  | GTP-binding protein rhoC  |

<sup>a</sup>Indicated significantly differential expression. SJ51\_C and SJ51M\_C represented without carbendazim treatment, while SJ51\_E and SJ51M\_E represented exposed to carbendazim treatment. The cut-off limit of DEGs was less than 0.05 FDR and greater than 2-fold change. -, no expression was detected in SJ51\_C and the expression abundance was very low in SJ51\_E

roles in mediating cellular resistance to the platinum compound [33]. The Rho GTPases subfamily plays crucial roles in regulating cytoskeletal organization and responding to extracellular growth factors [34]. The increased expression of FVER\_00402 (encoding GTP-binding protein rhoC) upon exposure of SJ51M to carbendazim suggested an important role for signal transduction mediated by small GTPases during stress conditions (Table 2).

Overexpression of drug target genes is also one mechanism that can confer resistance. This resistance mechanism involves a dose-effect, in which increased expression of the target gene can avoid saturation in the presence of a combination of fungicides [35]. Up-regulation of *Tub2* gene expression is associated with carbendazim resistance in *Paecilomyces lilacinus*, wherein the expression of *Tub2* is 4-fold higher than that in the wild type strain PI36-1 [28]. Here, FVER\_09254 expression was up-regulated by 2.7-fold in SJ51, but expression in SJ51M was similar in the presence or absence of carbendazim (Table 2). The compensation effect in SJ51 and the amino acid substitution Q134L in SJ51M might reduce the effects of a combination of carbendazim exposure and tubulin dysfunction.

A reduction in the concentration of toxic substances in cells mediated by overexpression of genes encoding detoxification enzymes and efflux transporters is correlated with drug resistance in several fungi [24, 36]. Cytochrome P450 monooxygenases (P450s) are known to mediate detoxification of fungicides, herbicide, pesticide and xenobiotics [37]. P450-mediated detoxification processes share common mechanisms and can also result in resistance of insects to insecticides [38, 39]. In a hypersensitive strain of *Candida albicans*, *CaALK8* (belonging to the CYP52 gene family) confers drug resistance [40]. The expressions of two genes (FVER\_05859 and FVER\_11192) related to CYP52 were up-regulated in SJ51M relative to wild type SJ51 (Table 2). Glutathione S-transferases (GSTs) involved in many essential cellular processes (e.g., xenobiotic detoxification, attenuation of oxidative stress, and signal transduction) have been reported to be associated with several resistance mechanisms. [41, 42] Our data showed that in the presence of carbendazim, the expressions of three genes (FVER\_00097, FVER\_08550 and FVER\_09899) encoding GST were up-regulated in resistant strain SJ51M relative to wild type SJ51. Remarkably, two major transmembrane transporters in fungal efflux systems (ABC transporters and MFS transporters) have been reported to modulate fungicide sensitivity and resistance [43, 44]. Substrates of these transporters include endogenous or exogenous toxic components, such as fungicides and secondary metabolites from the cell. Several genes encoding ABC multidrug transporters and MFS multidrug

transporters were identified from the transcriptome data (Table 2). Most were up-regulated in mutant SJ51M compared to wild type SJ51 in the presence of carbendazim treatment, especially the ABC multidrug transporters. A similar study was reported in the prochloraz-resistant strain HS-F6 [24]. Interestingly, genes related to drug detoxification and efflux transporters remained highly expressed after exposure to carbendazim even after continuous sub-culturing for 10 generations on fungicide-free PDA medium (in group SJ51M\_C vs SJ51\_C). These gene expression patterns might also occur under field conditions and could cause the rapid emergence of carbendazim resistant strains. The function of glyoxalase/bleomycin resistance protein/dioxygenase superfamily is to relieve the toxicity of methylglyoxal, a by-product of glycolysis [45]. The expression of two genes (FVER\_05972, FVER\_12450) associated with glyoxalase/bleomycin resistance protein/dioxygenase superfamily was intensely up-regulated in SJ51 and SJ51M after carbendazim treatment, especially in SJ51M (Table 2). It was speculated that this result might be related to dysfunctional energy metabolism in the presence of carbendazim and that the mutant SJ51M could have higher detoxification activity.

Expression of stress adaptation genes induced by exposure to drugs can overcome toxic effects and maintain cellular homeostasis that promotes survival. Many studies have demonstrated that cell stress responses and other mechanisms are associated with fungal resistance to azoles [46, 47]. The molecular chaperone heat shock 90 kDa protein (Hsp90) maintains protein stability to provide a critical mechanism for azole tolerance and resistance [48–50]. Here, expression of FVER\_10345, which encodes an Hsp90, was up-regulated in SJ51M in the presence of carbendazim (Table 2). Notably, expressions of many genes encoding other kinds of heat shock proteins, such as Hsp70 (FVER\_02883, FVER\_09674, FVER\_01860 and FVER\_11673) and Hsp104 (FVER\_04571), were also up-regulated in the SJ51M resistant mutant, indicating that many proteins were likely protected in the presence of carbendazim (Table 2). Similar results were observed for Hsp70 and Hsp104, which can induce protective responses to ketoconazole and amphotericin B in *Trichophyton rubrum* [51]. Expressions of two genes encoding thioredoxin and catalases were up-regulated in response to carbendazim in SJ51M. This up-regulation could protect the cell against oxidative stress and the accumulation of reactive oxygen species (ROS). These findings suggested that the mutant strain SJ51M could have higher viability following exposure to carbendazim. All these genes together enhanced survival of FSC exposed to carbendazim, and thus could be considered to be potential drug target genes.

## Conclusions

The results presented here showed that FSC were sensitive to carbendazim. Laboratory-induced resistant mutants obtained through carbendazim exposure indicated that FSC could quickly develop resistance to carbendazim. We identified two point mutations in the *Tub2* gene, including one novel point mutation from *F. proliferatum*, a temperature-susceptible FSC. Our results also provided a comprehensive analysis of mechanisms involved in FSC carbendazim resistance. By comparing transcriptome data for SJ51 and SJ51M with and without carbendazim treatment, genes related to carbendazim response and drug resistance were identified. These genes were involved in production of detoxification enzyme, drug efflux transporters as well as response to stress.

## Methods

### Sensitivity of FSC to carbendazim

Thirty-five single-spore isolates of FSC (Additional file 1: Table S1) were collected and recovered from 2012 to 2013 in the southern part of China that encompass major sugarcane production, including Fujian, Guangxi, Guangdong and Yunnan [8]. Carbendazim (97% a.i.; Yuanye; Shanghai, China) was dissolved in 0.1 M hydrochloric acid and adjusted to 10 mg a.i. mL<sup>-1</sup> as a stock solution to produce PDA medium (Hopebio; Qingdao, China) amended with 0, 0.5, 0.6, 0.7, 0.8, 0.9, 1.0, 1.1 or 1.2 µg a.i. mL<sup>-1</sup> carbendazim according to our preliminary results. A 5 mm diameter mycelial plug taken from the leading edge of a 3-day-old colony of each isolate was placed in the center of a 90 mm plate containing PDA medium amended with different carbendazim concentrations. Plates were incubated at 28 °C for 3 days in the dark, and the radial growth (colony diameter) of each isolate was measured in two perpendicular directions, with the original mycelial plug diameter (5 mm) subtracted from the measurement. Three replicate plates were used for each concentration and the experiment was repeated three times. For each isolate, the average radial colony growth was used to calculate the percent inhibition of mycelial growth and then a linear equation describing the percent inhibition of mycelial growth and the log<sub>10</sub> of the fungicide concentration of each isolate was obtained. [12, 52] The EC<sub>50</sub> was calculated according to the linear equation.

### Development of FSC mutants resistant to carbendazim in vitro

After measuring radial growth of colonies, the plates were used to obtain resistant mutants induced by carbendazim. Carbendazim-resistant mutants showed rapid growth in a fan-shaped region on the edge of the colony. The resistant phenotype strains in the fan-shaped region

were transferred to fungicide-free PDA medium and continuously sub-cultured for 10 generations [18, 28]. The sensitivity of resistant strains was measured as described above.

### Characteristics of carbendazim mutants

To determine temperature sensitivity, mutant strains and wild type counterparts were used to assess the ability to grow at various temperatures on PDA medium with or without carbendazim. A 5 mm diameter mycelial plug taken from the leading edge of a 3-day-old colony of each isolate was placed on a plate containing PDA medium amended with carbendazim at 0, 1.2 or 1.9 µg a.i. mL<sup>-1</sup>. Plates were incubated at 15 °C, 28 °C, 34 °C and 37 °C for 5 days in the dark, and the mycelial growth was recorded for each plate. Three replicate plates were used for each concentration and the experiment was performed three times. The radial growth (colony diameter) of each isolate cultured at 28 °C for 5 days without carbendazim treatment was measured in two perpendicular directions (with the original mycelial plug diameter subtracted from measurement) to analyze the fitness of mutants and the corresponding wild type strain. For pathogenicity assays, the conidia concentration of the wild type and mutants was adjusted to 1 × 10<sup>6</sup> conidia per mL. Each strain was micro-injected into 15 healthy sugarcane plants and injection of water was used as a control. The symptoms were observed at 10 days after injection.

### DNA extraction, cloning and sequence analysis of the *Tub2* gene

Three-day old mycelium from resistant mutants and wild type strains were cultured in PDB medium (Hopebio; Qingdao, China) and collected for extraction of DNA using the CTAB method [53]. The specific primers FVER\_05465F (5'-AGCGGCCAGTTAT TTCAGCA-3'), FVER\_05465R (5'-GCCGATTTCTCTCCTCCTT CTC-3'), FVER\_09254F (5'-TCCAATCCCTCTAG CCCTCG-3') and FVER\_09254R (5'-TCCTCGACA ACTTCACCACG-3') were designed to amplify complete coding sequence (CDS) of *Tub2* gene based on the genome sequence of *F. verticillioides* CNO-1. FPRO\_14041 and FPRO\_07779 are derived from the genome of *F. proliferatum* YN41 and the amplified primers are identical to the FVER\_09254 and FVER\_05465, respectively. Three biological replicates of each strain used for DNA extraction and the PCR reactions were conducted three times independently for each sample. The amplified PCR products were purified using a PCR Purification Kit (TIANGEN; Beijing, China), ligated into the pMD18-T Vector (TaKaRa Biotech; Dalian, China), and then sequenced by Sangon (Guangzhou, China). The exon sequences of the *Tub2* gene were

translated into amino acid sequences and aligned using DNAMAN8.0 software (Lynnon Biosoft; USA).

#### Total RNA extraction, construction of cDNA library and Illumina sequencing

To explore the molecular basis of carbendazim resistance, the highly resistant mutant SJ51M and its wild type counterpart SJ51 were used. A 5 mm diameter mycelial plug taken from the leading edge of each colony was aseptically transferred to 100 mL of PDB and cultured at 220 rpm for 48 h at 28 °C in the dark. Then, carbendazim at the EC<sub>50</sub> concentration (1.87 a.i. mL<sup>-1</sup> for SJ51M; 0.61 a.i. mL<sup>-1</sup> for SJ51) was added to the PDB medium. After 6 h incubation, the mycelia were collected, frozen in liquid nitrogen and stored at -80 °C. Untreated samples were used as a control.

Total RNA was extracted and purified from three biological replicates of each treatment resulting in 12 samples using Quick-RNATM Miniprep according to the manufacturer's instructions (Zymo Research, USA). The integrity and quality of the purified RNA were assessed by measuring the absorbance at 260/280 nm (A260/A280) and 1% agarose gel electrophoresis. To improve reliability and decrease the likelihood of biological error, equal amounts of total RNA from three biological replicates were pooled for Illumina deep RNA sequencing [23]. Sequencing libraries were constructed using NEB-Next® Ultra™ RNA Library Prep Kit for Illumina® (NEB, USA) according to the manufacturer's recommendations and index codes were added to attribute sequences to each sample. PCR products were purified (AMPure XP system) and the library quality was assessed on an Agilent Bioanalyzer 2100 system. Finally, the library preparations were sequenced on the Illumina HiSeq 2500 platform and paired-end reads were generated. Both library construction and sequencing were performed at BioMarker (Beijing, China).

#### Reads mapping to the reference genome

Raw data (raw reads) of fastq format were processed through in-house perl scripts. In this step, reads containing adapter, poly-N and low-quality reads were removed from the raw data to obtain clean reads that were then mapped to our sequenced genome *F. verticillioides* CNO-1 using Tophat software (V2.0) by default parameters [54]. Only reads with a perfect match or one mismatch were further analyzed and annotated based on the reference genome.

#### Gene expression analysis

DESeq provides statistical routines for determining differential expression in digital gene expression data using a model based on the negative binomial distribution.

Fragments Per Kilobase of exon model per Million fragments mapped (FPKM) were used to estimate gene expression levels. DEGs analysis of two groups was performed using the DESeq R package (1.10.1) [55]. The resulting *P* values were adjusted using Benjamini and Hochberg's approach for controlling the false discovery rate (FDR). Genes with FDR ≤ 0.05 and an absolute value of log<sub>2</sub> (fold change) ≥ 2 were set as the threshold for significantly differential expression. GO enrichment analysis of the DEGs was implemented using Goseq R packages based on Wallenius non-central hyper-geometric distribution, which can adjust for gene length bias in DEGs [56]. Kyoto Encyclopedia of Genes and Genomes (KEGG) pathway enrichment analysis of the DEGs was performed using KOBAS software [57].

#### qRT-PCR analysis

Total RNA (1 µg) from each sample was reverse transcribed using a PrimeScript™ RT reagent Kit with gDNA Eraser according to the manufacturer's instructions (TaKaRa; Dalian, China). Primers were designed using Oligo software v.7.37 and the specificity was confirmed by BLAST analysis against the *F. verticillioides* CNO-1 genome. The sequences of the primers are listed in Additional file 8: Table S6. All qRT-PCR reactions were conducted in a LightCycler 480 thermocycler (Roche) with a 20 µl reaction volume using SYBR® Premix Ex Taq™ II (TaKaRa; Dalian, China), as per the manufacturer's instructions. Melting curves were generated at the end of each PCR cycle to confirm the absence of nonspecific products in the reaction. Three biological replicate samples from each treatment were used for qRT-PCR analysis, and the reactions were performed in triplicate. To exclude the presence of contamination, a negative control containing no template (add sterile water) was included in all reactions. A 2<sup>-ΔΔCt</sup> algorithm was used to evaluate the relative fold change in the expression of the each gene using the *act1* (actin) gene as an endogenous control. [58, 59] The data were analyzed using LightCycler® 480 software version 1.5.1 (Roche). Pearson's correlation coefficients were calculated to evaluate the correlation of gene expression obtained by RNA-seq and qRT-PCR using Origin 9.0 software (Origin Lab).

#### Additional files

**Additional file 1: Table S1.** Carbendazim sensitivity of FSC isolates from sugarcane. The carbendazim EC<sub>50</sub> values for the 35 isolates ranged from 0.5097 to 0.6941 µg a.i. mL<sup>-1</sup> with an average EC<sub>50</sub> of 0.5957 µg a.i. mL<sup>-1</sup>. (DOCX 19 kb)

**Additional file 2: Table S2.** Carbendazim sensitivity of the resistant mutants. Five mutants had higher resistance to carbendazim with EC<sub>50</sub> over 1.0 µg a.i. mL<sup>-1</sup>, whereas another 13 mutants had EC<sub>50</sub> values that were similar to those for the wild type. (DOCX 17 kb)

**Additional file 3: Figure S1.** Alignments of the the *Tub2* amino acid sequences from resistant mutants and their wild-type strains. The consistent sequences are indicated by a blue background. The amino acid substitutions at positions: T351I between HC30 and HC30M over FPRO\_07779, and Q134L between SJ51 and SJ51M over FVER\_09254 were indicated by a white background. (JPG 945 kb)

**Additional file 4: Table S3.** Effects of temperature on mycelial growth of resistant mutants and their wild-types amended with carbendazim. After culturing for 5 days, SJ51M grew at all tested temperatures on PDA with carbendazim, but wild type SJ51 failed to grow. Neither the mutant HC30M nor its wild type counterpart HC30 grew at 15 °C on PDA medium with carbendazim but did grow on PDA without carbendazim. (DOCX 17 kb)

**Additional file 5: Figure S2.** Characteristics of carbendazim mutants and their wild types. Radial growth (A) and colony morphology (B) of carbendazim mutants and their wild types grown at 28 °C for 5 days. The radial growth (colony diameter) and colony morphology did not show significant difference of mutants SJ51M and HC30M compared with their wild types SJ51 and HC30. Error bars represent SD ( $n = 9$ ). (C) Pathogenicity test of the wild-types and their mutants. Each strain was inoculated by micro-injection with  $1 \times 10^6$  conidia  $\text{mL}^{-1}$ . The typical symptoms of growing point rot were observed after 10 days inoculation, while the control remained asymptomatic. Sterile water was used as a control. (TIF 2710 kb)

**Additional file 6: Table S4.** Percentages of reads mapped to the reference genome. TopHat2 tools soft were used to map with reference genome *F. verticillioides* CNO-1 by default parameters and over 75% of the total reads mapped to the genome. (DOCX 16 kb)

**Additional file 7: Table S5.** GO functional enrichment of the DEGs in SJ51M and its corresponding wild type strain SJ51. SJ51\_C and SJ51M\_C represented without carbendazim treatment, while SJ51\_E and SJ51M\_E represented exposed to carbendazim treatment. (XLSX 47 kb)

**Additional file 8: Table S6.** List of primers used for the qRT-PCR analysis. Ten genes related to transmembrane transport, oxidoreductase activity, response to stress and the target gene of carbendazim were validated via qRT-PCR analysis. (DOCX 16 kb)

## Abbreviations

a.i.: active ingredient; CDS: coding sequence; DEGs: differentially expressed genes;  $\text{EC}_{50}$ : the fungicide concentration that inhibits 50% of mycelial growth; FDR: false discovery rate; FPKM: fragments per kilobase of exon model per million fragments mapped; FSC: *Fusarium* species complex; GO: gene ontology; GST: glutathione S-transferase; Hsp: heat shock protein; KEGG: Kyoto Encyclopedia of Genes and Genomes; MBC: methyl benzimidazole carbamate; MFS: major facilitator superfamily; P450s: cytochrome P450 monooxygenases; PDA: potato dextrose agar; PDB: potato dextrose broth; qRT-PCR: quantitative real-time PCR; RNA-seq: RNA sequencing; ROS: reactive oxygen species; SRA: Sequence Read Archive; *Tub2*:  $\beta$ -tubulin 2

## Acknowledgments

We especially thank Bioscience Editing Solutions for critical reading of the manuscript and useful comments.

## Funding

This work was supported by the National Natural Science Foundation of China (31460374), the Key Project of Science and Technology of Guangxi (AA17202042–7), and Scientific Foundation of State Key Laboratory for Conservation and Utilization of Subtropical Agro-bioresources (SKLCUSA-a201805).

## Availability of data and materials

The sequencing data are available through the Sequence Read Archive in the GenBank database under accession number SRP127969 with the following link: <https://www.ncbi.nlm.nih.gov/sra/SRP127969>. GO functional enrichment of the DEGs in different samples are provided in the Additional file 7.

## Authors' contributions

ZMQ, CBS, XSQ and WJH designed the research. XSQ, WJH, WHX and LYS performed the experiments. ZMQ, CBS, YW, BYX and MG provided guidance on the data analysis. XSQ, WJH and ZMQ wrote the manuscript. All authors read

and approved the final manuscript. Each author have participated sufficiently in the work and made substantial contributions throughout the research.

## Ethics approval and consent to participate

Not applicable.

## Consent for publication

Not applicable.

## Competing interests

The authors declare that they have no competing interests.

## Publisher's Note

Springer Nature remains neutral with regard to jurisdictional claims in published maps and institutional affiliations.

## Author details

<sup>1</sup>State Key Lab for Conservation and Utilization of Subtropical Agric-Biological Resources, Guangxi University, Nanning 530005, China. <sup>2</sup>Crop Research Institute of Guangdong Academy of Agricultural Science, Guangzhou 510640, China.

Received: 25 June 2018 Accepted: 24 January 2019

Published online: 07 February 2019

## References

- Rott P. A guide to sugarcane diseases: editions quae; 2000.
- Vishwakarma S, Kumar P, Nigam A, Singh A, Kumar A. Pokkah boeng: an emerging disease of sugarcane. *J Plant Pathol Microbiol.* 2013;4(170):2.
- Singh A, Chauhan S, Singh A, Singh S. Deterioration in sugarcane due to pokkah boeng disease. *Sugar Tech.* 2006;8(2–3):187–90.
- Shan H, Li W, Zhang R, Wang X, Li J, Cang X, Yin J, Luo Z, Huang Y. Analysis on epidemic reason of sugarcane pokkah boeng and its losses on yield and sucrose content. *Sugar Crops China.* 2018;03(40):40–2.
- McFarlane S, Rutherford R. *Fusarium* species isolated from sugarcane in KwaZulu-Natal and their effect on *Eldana saccharina* (Lepidoptera: Pyralidae) development in vitro. In: *Proc S Afr Sug Technol ass: 2005; 2005.* p. 120–4.
- Siddique S. Pathogenicity and aethiology of *Fusarium* species associated with pokkah boeng disease on sugarcane. In: *Dissertation University of Malaysia; 2007.*
- Viswanathan R, Poongothai M, Malathi P. Pathogenic and molecular confirmation of *Fusarium sacchari* causing wilt in sugarcane. *Sugar Tech.* 2011;13(1):68–76.
- Lin Z, Xu S, Que Y, Wang J, Comstock JC, Wei J, McCord PH, Chen B, Chen R, Zhang M. Species-specific detection and identification of fusarium species complex, the causal agent of sugarcane pokkah boeng in China. *PLoS One.* 2014;9(8):e104195.
- Karuppaiyan R, Ram B, Ramdiya S, Ali M, Meena M. The incidence of pokkah boeng in indigenous and exotic sugarcane (*Saccharum officinarum*) clones. *Indian J Agric Sci.* 2015;85(4):596–601.
- Davidse L. Antimitotic activity of methyl benzimidazol-2-yl carbamate (MBC) in *Aspergillus nidulans*. *Pestic Biochem Physiol.* 1973;3(3):317–25.
- Russell P. Fungicide resistance: occurrence and management. *J Agric Sci.* 1995;124(3):317–23.
- Ma Z, Yoshimura MA, Michailides TJ. Identification and characterization of benzimidazole resistance in *Monilinia fructicola* from stone fruit orchards in California. *Appl Environ Microbiol.* 2003;69(12):7145–52.
- Albertini C, Gredt M, Leroux P. Mutations of the  $\beta$ -tubulin gene associated with different phenotypes of benzimidazole resistance in the cereal eyespot fungi *Tapesia yallundae* and *Tapesia acuformis*. *Pestic Biochem Physiol.* 1999;64(1):17–31.
- Zhang H, Brankovics B, van der Lee TA, Waalwijk C, van Diepeningen AA, Xu J, Xu J, Chen W, Feng J. A single-nucleotide-polymorphism-based genotyping assay for simultaneous detection of different carbendazim-resistant genotypes in the *Fusarium graminearum* species complex. *PeerJ.* 2016;4:e2609.
- Bollen GJ, Scholten G. Acquired resistance to benomyl and some other systemic fungicides in a strain of *Botrytis cinerea* in cyclamen. *Neth J Plant Pathol.* 1971;77(3):83–90.

16. Ma Z, Michailides TJ. Advances in understanding molecular mechanisms of fungicide resistance and molecular detection of resistant genotypes in phytopathogenic fungi. *Crop Prot.* 2005;24(10):853–63.
17. Koenraad H, Somerville SC, Jones A. Characterization of mutations in the beta-tubulin gene of benomyl-resistant field strains of *Venturia inaequalis* and other plant pathogenic fungi. *Phytopathology.* 1992;82(11):1348–54.
18. Sevastos A, Markoglou A, Labrou N, Flouri F, Malandrakis A. Molecular characterization, fitness and mycotoxin production of *Fusarium graminearum* laboratory strains resistant to benzimidazoles. *Pestic Biochem Physiol.* 2016;128:1–9.
19. Chen Z, Gao T, Liang S, Liu K, Zhou M, Chen C. Molecular mechanism of resistance of *Fusarium fujikuroi* to benzimidazole fungicides. *FEMS Microbiol Lett.* 2014;357(1):77–84.
20. Kawchuk L, Hutchison L, Verhaeghe C, Lynch D, Bains P, Holley J. Isolation of the  $\beta$ -tubulin gene and characterization of thiabendazole resistance in *Gibberella pulicaris*. *Can J Plant Pathol.* 2002;24(2):233–8.
21. Suga H, Nakajima T, Kageyama K, Hyakumachi M. The genetic profile and molecular diagnosis of thiophanate-methyl resistant strains of *Fusarium asiaticum* in Japan. *Fungal biology.* 2011;115(12):1244–50.
22. Martinez-Rossi NM, Peres NT, Rossi A. Antifungal resistance mechanisms in dermatophytes. *Mycopathologia.* 2008;166(5–6):369–83.
23. Persinoti GF, de Aguiar Peres NT, Jacob TR, Rossi A, Vêncio RZ, Martinez-Rossi NM. RNA-sequencing analysis of *Trichophyton rubrum* transcriptome in response to sublethal doses of acriflavine. *BMC Genomics.* 2014;15(7):S1.
24. Liu J, Wang S, Qin T, Li N, Niu Y, Li D, Yuan Y, Geng H, Xiong L, Liu D. Whole transcriptome analysis of *Penicillium digitatum* strains treated with prochloraz reveals their drug-resistant mechanisms. *BMC Genomics.* 2015;16(1):855.
25. Zhang M, Jeyakumar JM. *Fusarium* Species Causing Pokkah Boeng in China. In: *Fusarium-Plant Disease, Pathogen Diversity, Genetic Diversity, Resistance and Molecules.* Edited by Tulin Askun. Intech Open. 2018. <https://doi.org/10.5772/intechopen.73133>.
26. Liu X, Yin Y, Wu J, Jiang J, Ma Z. Identification and characterization of carbendazim-resistant isolates of *Gibberella zeae*. *Plant Dis.* 2010;94(9):1137–42.
27. Wu W, Li R, Zheng F. Identification and toxicity indoor of the pathogens causing Pokkah Boeng disease of sugarcane. *Sugarcane Canesugar.* 2006;2:10–4.
28. Yang F, Abdelnabby H, Xiao Y. Novel point mutations in  $\beta$ -tubulin gene for carbendazim resistance maintaining nematode pathogenicity of *Paecilomyces lilacinus*. *Eur J Plant Pathol.* 2015;143(1):57–68.
29. Newcombe G, Thomas P. Inheritance of carboxin resistance in a European field isolate of *Ustilago nuda*. *Phytopathology.* 2000;90(2):179–82.
30. Avenot HF, Michailides TJ. Resistance to boscalid fungicide in *Alternaria alternata* isolates from pistachio in California. *Plant Dis.* 2007;91(10):1345–50.
31. Mandelkow E, Hoenger A. Structures of kinesin and kinesin-microtubule interactions. *Curr Opin Cell Biol.* 1999;11(1):34–44.
32. Zheng Z, Hou Y, Cai Y, Zhang Y, Li Y, Zhou M. Whole-genome sequencing reveals that mutations in myosin-5 confer resistance to the fungicide phenamacril in *Fusarium graminearum*. *Sci Rep.* 2015;5:8248.
33. Shen D-W, Pouliot LM, Hall MD, Gottesman MM. Cisplatin resistance: a cellular self-defense mechanism resulting from multiple epigenetic and genetic changes. *Pharmacol Rev.* 2012;64(3):706–21.
34. Van Aelst L, D'Souza-Schorey C. Rho GTPases and signaling networks. *Genes Dev.* 1997;11(18):2295–322.
35. Sanglard D, Coste A, Ferrari S. Antifungal drug resistance mechanisms in fungal pathogens from the perspective of transcriptional gene regulation. *FEMS Yeast Res.* 2009;9(7):1029–50.
36. Andrade AC, Del Sorbo G, Van Nistelrooy JG, De Waard MA. The ABC transporter AtrB from *Aspergillus nidulans* mediates resistance to all major classes of fungicides and some natural toxic compounds. *Microbiology.* 2000;146(8):1987–97.
37. Črešnar B, Petrič S. Cytochrome P450 enzymes in the fungal kingdom. *Biochimica et Biophysica Acta (BBA)-Proteins and Proteomics.* 2011; 1814(1):29–35.
38. Scott JG. Cytochromes P450 and insecticide resistance. *Insect Biochem Mol Biol.* 1999;29(9):757–77.
39. Karunker I, Benting J, Lueke B, Ponge T, Nauen R, Roditakis E, Vontas J, Gorman K, Denholm I, Morin S. Over-expression of cytochrome P450 CYP6CM1 is associated with high resistance to imidacloprid in the B and Q biotypes of *Bemisia tabaci* (Hemiptera: Aleyrodidae). *Insect Biochem Mol Biol.* 2008;38(6):634–44.
40. Lata Panwar S, Krishnamurthy S, Gupta V, Alarco AM, Raymond M, Sanglard D, Prasad R. CaALK8, an alkane assimilating cytochrome P450, confers multidrug resistance when expressed in a hypersensitive strain of *Candida albicans*. *Yeast.* 2001;18(12):1117–29.
41. Cohen E, Gamliel A, Katan J. Glutathione and glutathione-S-transferase in fungi: effect of pentachloronitrobenzene and 1-chloro-2, 4-dinitrobenzene; purification and characterization of the transferase from *Fusarium*. *Pestic Biochem Physiol.* 1986;26(1):1–9.
42. Ortelli F, Rossiter LC, Vontas J, Ranson H, Hemingway J. Heterologous expression of four glutathione transferase genes genetically linked to a major insecticide-resistance locus from the malaria vector *Anopheles gambiae*. *Biochem J.* 2003;373(3):957–63.
43. Del Sorbo G, Schoonbeek H-J, De Waard MA. Fungal transporters involved in efflux of natural toxic compounds and fungicides. *Fungal Genet Biol.* 2000;30(1):1–15.
44. Deising HB, Reimann S, Pascholati SF. Mechanisms and significance of fungicide resistance. *Braz J Microbiol.* 2008;39(2):286–95.
45. Töwe S, Leelakriangsak M, Kobayashi K, Van Duy N, Hecker M, Zuber P, Antelmann H. The MarR-type repressor MhqR (YkvE) regulates multiple dioxygenases/glyoxalases and an azoreductase which confer resistance to 2-methylhydroquinone and catechol in *Bacillus subtilis*. *Mol Microbiol.* 2007; 66(1):40–54.
46. Cowen LE, Sanglard D, Howard SJ, Rogers PD, Perlin DS. Mechanisms of antifungal drug resistance. *Cold Spring Harbor perspectives in medicine.* 2015;5(7):a019752.
47. Shapiro RS, Robbins N, Cowen LE. Regulatory circuitry governing fungal development, drug resistance, and disease. *Microbiol Mol Biol Rev.* 2011; 75(2):213–67.
48. Cowen LE. Hsp90 orchestrates stress response signaling governing fungal drug resistance. *PLoS Pathog.* 2009;5(8):e1000471.
49. Shapiro RS, Zaas AK, Betancourt-Quiroz M, Perfect JR, Cowen LE. The Hsp90 co-chaperone Sgt1 governs *Candida albicans* morphogenesis and drug resistance. *PLoS One.* 2012;7(9):e44734.
50. Robbins N, Uppuluri P, Nett J, Rajendran R, Ramage G, Lopez-Ribot JL, Andes D, Cowen LE. Hsp90 governs dispersion and drug resistance of fungal biofilms. *PLoS Pathog.* 2011;7(9):e1002257.
51. Yu L, Zhang W, Wang L, Yang J, Liu T, Peng J, Leng W, Chen L, Li R, Jin Q. Transcriptional profiles of the response to ketoconazole and amphotericin B in *Trichophyton rubrum*. *Antimicrob Agents Chemother.* 2007;51(1):144–53.
52. Qiu J, Xu J, Yu J, Bi C, Chen C, Zhou M. Localisation of the benzimidazole fungicide binding site of *Gibberella zeae*  $\beta$ 2-tubulin studied by site-directed mutagenesis. *Pest Manag Sci.* 2011;67(2):191–8.
53. Möller E, Bahnweg G, Sandermann H, Geiger H. A simple and efficient protocol for isolation of high molecular weight DNA from filamentous fungi, fruit bodies, and infected plant tissues. *Nucleic Acids Res.* 1992;20(22):6115–6.
54. Kim D, Perteu G, Trapnell C, Pimentel H, Kelley R, Salzberg SL. TopHat2: accurate alignment of transcriptomes in the presence of insertions, deletions and gene fusions. *Genome Biol.* 2013;14(4):R36.
55. Wang L, Feng Z, Wang X, Wang X, Zhang X. DESeq: an R package for identifying differentially expressed genes from RNA-seq data. *Bioinformatics.* 2009;26(1):136–8.
56. Young MD, Wakefield MJ, Smyth GK, Oshlack A. Gene ontology analysis for RNA-seq: accounting for selection bias. *Genome Biol.* 2010;11(2):R14.
57. Mao X, Cai T, Olyarchuk JG, Wei L. Automated genome annotation and pathway identification using the KEGG Orthology (KO) as a controlled vocabulary. *Bioinformatics.* 2005;21(19):3787–93.
58. Lin Z, Wang J, Bao Y, Guo Q, Powell CA, Xu S, Chen B, Zhang M. Deciphering the transcriptomic response of *Fusarium verticillioides* in relation to nitrogen availability and the development of sugarcane pokkah boeng disease. *Sci Rep.* 2016;6:29692.
59. Livak KJ, Schmittgen TD. Analysis of relative gene expression data using real-time quantitative PCR and the  $2^{-\Delta\Delta CT}$  method. *Methods.* 2001;25(4):402–8.